Distributed feedback laser biosensor incorporating a titanium dioxide nanorod surface

Chun Ge,[1] Meng Lu,[1] Wei Zhang,[2] and Brian T. Cunningham[1,3,a)]
[1]*Department of Electrical and Computer Engineering, University of Illinois at Urbana-Champaign, Urbana, Illinois 61801, USA*
[2]*Department of Materials Science and Engineering, University of Illinois at Urbana-Champaign, Urbana, Illinois 61801, USA*
[3]*Department of Bioengineering, University of Illinois at Urbana-Champaign, Urbana, Illinois 61801, USA*

(Received 1 January 2010; accepted 23 March 2010; published online 19 April 2010)

A dielectric nanorod structure is used to enhance the label-free detection sensitivity of a vertically-emitting distributed feedback laser biosensor (DFBLB). The device is comprised of a replica molded plastic grating that is subsequently coated with a dye-doped polymer layer and a TiO_2 nanorod layer produced by the glancing angle deposition technique. The DFBLB emission wavelength is modulated by the adsorption of biomolecules, whose greater dielectric permittivity with respect to the surrounding liquid media will increase the laser wavelength in proportion to the density of surface-adsorbed biomaterial. The nanorod layer provides greater surface area than a solid dielectric thin film, resulting in the ability to incorporate a greater number of molecules. The detection of a monolayer of protein polymer poly (Lys, Phe) is used to demonstrate that a 90 nm TiO_2 nanorod structure improves the detection sensitivity by a factor of 6.6 compared to an identical sensor with a nonporous TiO_2 surface. © *2010 American Institute of Physics*.
[doi:10.1063/1.3394259]

Label-free optical biosensors based upon detection of transmitted or reflected spectra from passive optical resonators have found many applications in life science research, environmental monitoring, quality control testing, pharmaceutical drug discovery, and diagnostic testing.[1–4] Resonant optical structures such as photonic crystal surfaces,[1,2] silicon oxide ring resonators,[5] thin-walled glass capillaries,[6–8] and microtoroids[9] generally detect resonant wavelength shift due to the interaction between captured target molecules and the evanescent electric field of the resonant modes, where the amount of wavelength shift is proportional to the density of immobilized biomaterial on the sensor surface. Such sensors are designed to have extremely smooth surfaces to minimize optical losses due to scattering in order to maintain a high *Q*-factor for wavelength resolution. Recently, optical biosensors based upon distributed feedback (DFB) lasers fabricated upon plastic surfaces have been demonstrated as active optical resonators that obtain high *Q*-factor through the process of stimulated emission. Operating with single mode, narrow linewidth emission,[10–16] DFB laser biosensors (DFBLBs) are simultaneously capable of high sensitivity and a high degree of resolution. In previous work, we have demonstrated DFBLBs that incorporate a thin solid film of TiO_2 as the uppermost surface, where a 40–80 nm thick layer of TiO_2 serves to bias the resonant mode to reside more fully within the liquid media in contact with the DFBLB surface, thus providing a strong dependency of the emission wavelength on the density of adsorbed biomolecules.[16]

Here, we demonstrate that a nanostructured TiO_2 layer may be used in place of a thin solid film of TiO_2. We show that the use of the nanostructured film results in a three-dimensional volume overlap between the DFBLB resonant mode and the region where biomolecule adsorption can occur. This modification in device design results in a 6.6× increase in detection sensitivity, while at the same time maintaining a narrow spectral output, with cavity quality factor Q=25 and 600. The TiO_2 nanorod structure was deposited by e-beam evaporation using the glancing angle deposition (GLAD) method in which the incident material flux is provided at an oblique angle to the device surface.[17–19]

As shown in Fig. 1, the DFBLB structure is comprised of a low refractive index ultraviolet curable polymer (UVCP) grating (n=1.38, period=400 nm, and depth=160 nm) that is overcoated with a thin film of SU-8 (5.0 wt %; Microchem, n=1.58 and t=400 nm) that is doped with a laser dye (Rhomamine 590, Exciton) as described in previous work.[16] The grating structure is fabricated using nanoreplica molding using a silicon wafer with a negative image of the DFBLB grating structure as a template. A small volume (~1 ml) of liquid UVCP is spread between the silicon template wafer and a flexible sheet of polyester film with a cylindrical roller,

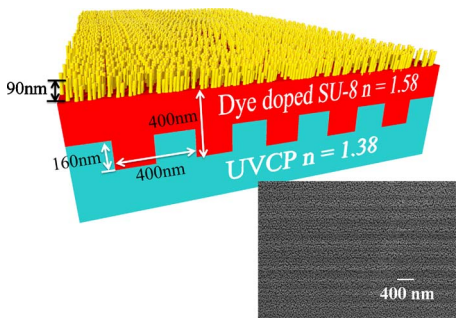

FIG. 1. (Color online) Cross-sectional diagram of the DFBLB structure (not to scale). The period and depth of the grating structure are 400 nm and 160 nm, respectively. The sensor surface was coated with TiO_2 nanorod film with thickness of 90 nm. A top-view SEM image of the nanorod coated sensor is also shown.

a)Author to whom correspondence should be addressed. Electronic mail: bcunning@illinois.edu.

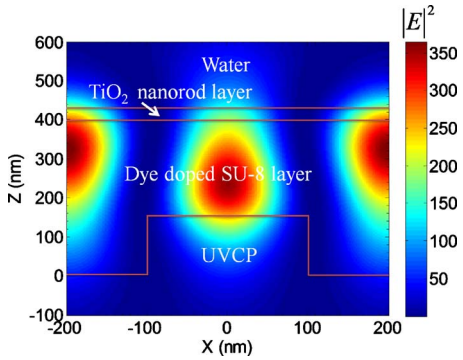

FIG. 2. (Color online) Electric field intensity profile for a DFBLB with a 30 nm TiO_2 nanorod film.

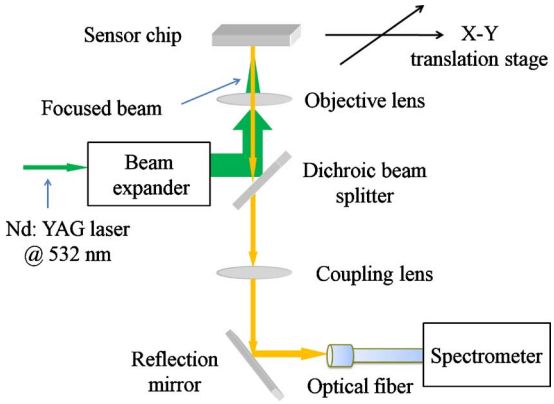

FIG. 3. (Color online) Schematic of the biosensor detection instrument setup.

enabling the liquid polymer to fill the silicon grating surface. The polymer film is cured to a solid with exposure to a high intensity ultraviolet lamp (Xenon) for ~90 s, and the resulting grating structure is peeled away from the silicon wafer, resulting in $\sim 12 \times 9$ cm^2 DFBLB continuous grating surfaces. The polymer grating structure was treated by oxygen plasma for 50 s to improve the adhesion of the SU-8/dye layer, which is applied by spin coating (4000 rpm and 35 s). The SU-8/dye layer provides optical gain while at the same time providing vertical light confinement and horizontal feedback.

The TiO_2 nanorod layer is deposited on top of the SU-8/dye layer by the GLAD technique. All GLADs were performed at a base pressure of 3.0×10^{-6} Torr and deposition rate of 7.2 Å/s. A scanning electron microscope (SEM) image of a GLAD TiO_2 film deposited upon a DFBLB is shown in Fig. 1. A steady-state electric-field intensity cross-section profile at resonance was calculated using rigorous coupled-wave analysis (RCWA) for a device with a 30 nm TiO_2 nanorod coating, as shown in Fig. 2. The superstrate was water ($n=1.33$) and an effective refractive index of $n=1.82$ was used for the TiO_2 nanorod layer when immersed in water. The polarization of the calculated electrical field is parallel to the grating (TE polarization). The TE polarization is selected because the fundamental lasing mode is TE_0 mode. When the thickness of the TiO_2 nanorod layer is increased, the electromagnetic field distribution is altered, but only very slightly because the thickness of the TiO_2 nanorod layer ($22\ \text{nm} < t < 90\ \text{nm}$), is a small perturbation of the structure when compared to the dye doped SU-8 layer ($t \sim 400$ nm).[20]

As shown in Fig. 3, the DFBLB was pumped by a 10 ns Q-switched Nd:yttrium aluminum garnet (YAG) laser pulses at $\lambda = 532$ nm. The pump light first goes through a spatial filter, and then is expanded and focused onto the sensor through a 20× microscope objective ($f=9$ mm) placed beneath the senor. The laser emission is collected with an optical fiber (diameter=0.5 mm) and delivered to a charge-coupled device based spectrometer with 0.0125 nm resolution (Horiba Jobin Yvon iHR550). The DFB cavity demonstrated in this letter is based on a second order Bragg grating that supports a vertically emitting mode by first-order diffraction. Lasing occurs at the one band edge near the Bragg resonance, determined by the equation $m\lambda_{\text{Bragg}} = 2n_{\text{eff}}\Lambda$, where $m=2$ is the order of diffraction, n_{eff} is the effective refractive index of the resonant mode, and Λ is the grating period. The diameter of the excitation spot is ~100 μm. During the DFB laser operation (<10 ns per pulse), the local temperature variation caused by light absorption is negligible using a pumping rate of 4 Hz and a pumping fluence of 25 $\mu J/mm^2$. Assuming that ~15% of the pump energy is absorbed by the laser, the time averaged pumping power absorbed by sensor chip is only 15 $\mu W/mm^2$, and the actual optical power converted to thermal power is even lower than this value. Therefore, the pumping laser-induced heating effects are negligible.

The DFBLB sheet is attached to a bottomless 96-well microplate with adhesive, so the DFBLB forms the entire bottom surface of each 6.7 mm diameter microplate well. The biosensor microplate is held in a fixture that is attached to an x-y motion stage, which enables computer-programmed excitation of a precise location on the DFB surface. Within a single microplate well, the excitation laser separately probes 75 independent locations in an x-y rectangular grid with 400 μm spacing to compute the average PWV. Gathering the 75 measurements takes ~60 s.

Figure 4 shows the laser emission spectrum of a DFBLB with a $t=90$ nm nanorod coating and with sensor surface immersed in water. The observed lasing wavelength is at $\lambda = 602.4513$ nm and the full width half maximum (FWHM) is $\Delta\lambda \sim 0.0235$ nm, corresponding to a Q factor of 25 600. Here, both peak wavelength value (PWV) and FWHM of the emission spectrum are obtained by fitting the discrete measurements from the spectrometer with a Lorentzian model, enabling a peak fitting algorithm to obtain PWV shift resolution lower than the spectrometer resolution. The inset of Fig. 4 shows the dependence of the laser emission wave-

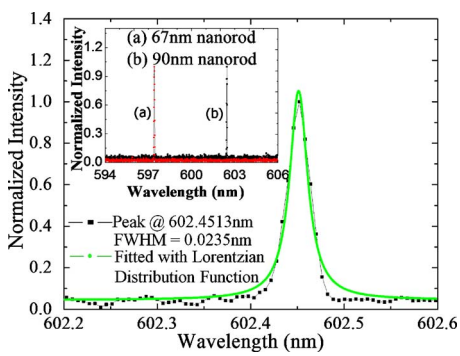

FIG. 4. (Color online) DFB laser emission profile. The sensor was coated with 90 nm TiO_2 nanorod film and immersed in DI water. Inset shows the redshift in PWV due to increased TiO_2 nanorod thickness.

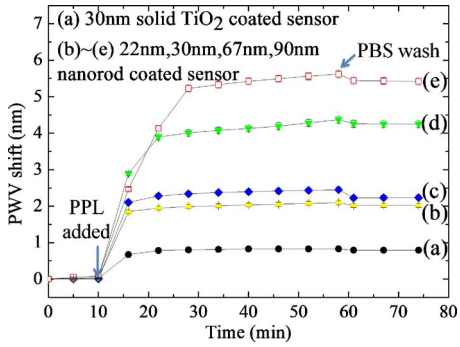

FIG. 5. (Color online) Dynamic detection of adsorption of a polymer protein self-limiting monolayer for nonporous TiO_2 film coated and porous TiO_2 nanorod coated sensors.

length as a function of nanorod thickness. The TiO_2 nanorod layer causes the PWV to shift to longer wavelength. Meanwhile, the linewidth of the emission spectrum remains as narrow as the DFB structure without a nanorod TiO_2 film coating. This indicates that the nanorods, with feature size far below the resonant wavelength of $\lambda \sim 600$ nm, do not cause scattering or absorption that results in a measurable effect other than the addition of material with higher dielectric permittivity than water.

To demonstrate the sensitivity enhancement resulting from the TiO_2 nanorod layer, sensitivity to surface mass adsorption was characterized. Sensors with either a 30 nm solid TiO_2 film or nanorod TiO_2 films of 22, 30, 67, and 90 nm were prepared. All the sensors were coated with a single monolayer of protein using the following protocol. First, the sensors were exposed to a phosphate buffered saline (PBS) solution for 10 min, after which a baseline PWV measurement was taken from each biosensor microplate well, as described above. Next, the PBS solution was removed by pipette and the wells were refilled with 1 mg/ml solution of the protein polymer poly (Lys, Phe) (PPL, Sigma-Aldrich). In previous research, PPL has been demonstrated to form a self-limiting single monolayer coating upon dielectric surfaces.[10] PPL molecules have a molecular weight of 35 400 Da and a linear chain structure, and are therefore expected to penetrate the TiO_2 nanorod layer and to result in binding that is proportional to the available exposed surface area. Previous characterization of PPL films estimated that the film thickness is ~15 nm with a refractive index of ~1.45.[10] The PPL solution was incubated with the sensor surfaces for 48 min, after which the PPL solution was removed and the sensor surface was rinsed with PBS solution three times to remove any PPL that was not firmly attached. With PBS solution in the biosensor microplate wells, a second set of PWV measurements were gathered. Each active biosensor microplate well exposed to PPL was accompanied by a reference well that was not exposed to PPL, in order to compensate for any possible common mode experimental artifacts during the PPL incubation step. The PWV shift reported in Fig. 5 represents the wavelength shift difference between the active sensor and its reference. Overall, the reference sensor supplied very little correction, as no reference sensor had a shift in greater than 0.0283 nm during the incubation step. Our results show that thicker TiO_2 nanorod films result in greater PWV shift for adsorption of PPL, and the thickest nanorod layer (90 nm) results in a 6.6× enhancement in surface sensitivity. Importantly, as shown by the kinetic binding plots in Fig. 5, the 90 nm nanorod film does not appear to substantially limit the rate of monolayer adsorption, as the nanorod spacings are large enough to enable PPL molecules to enter without an evident diffusion limitation. Because the DFB lasing mode is predicted by RCWA models (not shown) to extend only ~100 nm into the nanorod layer, thicknesses of this magnitude are expected to optimize the PWV shift. Greater thickness of the nanorod layer will increase the available surface area, but at a cost of more difficult diffusion of molecules to the regions closest to the SU-8 upper surface, where interaction between adsorbed molecules and the resonant mode electric field is greatest.

This project was made possible by a cooperative agreement that was awarded and administered by the U.S. Army Medical Research & Materiel Command (USAMRMC) and the Telemedicine & Advanced Technology Research Center (TATRC), under Contract No. W81XWH0810701.

[1]B. T. Cunningham, P. Li, S. Schulz, B. Lin, C. Baird, J. Gerstenmaier, C. Genick, F. Wang, E. Fine, and L. Laing, J. Biomol. Screening **9**, 481 (2004).
[2]B. T. Cunningham and L. L. Laing, Expert Rev. Proteomics **3**, 271 (2006).
[3]R. Narayanaswamy and O. S. Wolfbeis, *Optical Sensors: Industrial, Environmental and Diagnostic Applications* (Springer, Berlin, 2004).
[4]A. J. Cunningham, *Introduction to Bioanalytical Sensors* (Wiley, New York, 1998).
[5]A. L. Washburn, L. C. Gunn, and R. C. Bailey, Anal. Chem. **81**, 9499 (2009).
[6]I. M. White, H. Oveys, X. Fan, T. L. Smith, and J. Zhang, Appl. Phys. Lett. **89**, 191106 (2006).
[7]H. Zhu, I. M. White, J. D. Suter, P. S. Dale, and X. Fan, Opt. Express **15**, 9139 (2007).
[8]J. D. Suter, I. M. White, H. Zhu, H. Shi, C. W. Caldwell, and X. Fan, Biosens. Bioelectron. **23**, 1003 (2008).
[9]A. M. Armani, R. P. Kulkarni, S. E. Fraser, R. C. Flagan, and K. J. Vahala, Science **317**, 783 (2007).
[10]M. Lu, S. Choi, C. J. Wagner, J. G. Eden, and B. T. Cunningham, Appl. Phys. Lett. **92**, 261502 (2008).
[11]C. Henry, R. Kazarinov, R. Logan, and R. Yen, IEEE J. Quantum Electron. **21**, 151 (1985).
[12]S. Balslev, T. Rasmussen, P. Shi, and A. Kristensen, J. Micromech. Microeng. **15**, 2456 (2005).
[13]R. Kazarinov and C. Henry, IEEE J. Quantum Electron. **21**, 144 (1985).
[14]H. Temkin, G. J. Dolan, R. A. Logan, R. F. Kazarinov, N. A. Olsson, and C. H. Henry, Appl. Phys. Lett. **46**, 105 (1985).
[15]Y. Chen, Z. Li, Z. Zhang, D. Psaltis, and A. Scherer, Appl. Phys. Lett. **91**, 051109 (2007).
[16]M. Lu, S. S. Choi, U. Irfan, and B. T. Cunningham, Appl. Phys. Lett. **92**, 111113 (2008).
[17]W. Zhang, N. Ganesh, P. C. Mathias, and B. T. Cunningham, Small **4**, 2199 (2008).
[18]K. Robbie, L. J. Friedrich, S. K. Dew, T. Smy, and M. J. Brett, J. Vac. Sci. Technol. A **13**, 1032 (1995).
[19]W. Zhang, N. Ganesh, I. D. Block, and B. T. Cunningham, Sens. Actuators B **131**, 279 (2008).
[20]I. D. Block, N. Ganesh, M. Lu, and B. T. Cunningham, IEEE Sens. J. **8**, 274 (2008).